

The dynamics of the flat anisotropic models in the Lovelock gravity.

I: The even-dimensional case

S.A. Pavluchenko

Special Astrophysical Observatory, Russian Academy of Sciences, Nizhnij Arkhyz, 369167 Russia

In this article we give a full description of the dynamics of the flat anisotropic (4+1)-dimensional cosmological model in the presence of both Gauss-Bonnet and Einstein contributions. This is the first complete description of this model with both terms taken into account. Our data is obtained using the numerical analysis, though, we use analytics to explain some features of the results obtained, and the same analytics could be applied to higher-dimensional models in higher-order Lovelock corrections. Firstly, we investigate the vacuum model and give a description of all regimes; then, we add a matter source in the form of a perfect fluid and study the influence the matter exerts upon the dynamics. Thus, we give a description of matter regimes as well. Additionally, we demonstrate that the presence of matter not only “improves” the situation with a smooth transition between the standard singularity and the Kasner regime, but also brings additional regimes and even partially “erases” the boundaries between different regimes inside the same triplet. Finally, we discuss the numerical and analytical results obtained and their generalization to the higher-order models.

PACS numbers: 04.20.Dw, 04.25.dc, 04.50.-h, 04.50.Kd, 98.80.-k

I. INTRODUCTION

The idea of extra dimensions traces back to the beginning of last century, to the papers by Nordström [1], Kaluza [2] and Klein [3]. At that time such ideas were considered as mere mathematical speculations, but with time they have come to hold a firm place in the minds of scientists. The 70s gave rise to an interest in the extradimensional theories due to the development of superstring and supergravity theories (see, e.g., [4]). Later in the 90s the interest has only increased owing to the possibility to solve the hierarchy problem [5], lower the grand unification scale in the M-theory [6] and in many others (see, e.g., [7] for recent reviews).

Dealing with extra dimensions in the cosmological context, one usually uses a modified gravity (see the forementioned reviews). One of modifications of this kind is the Lovelock gravity [8]. This theory is equivalent to Einstein’s theory in (3+1), but starting from (4+1) it gives rise to

higher-order (in powers of curvature) corrections. The first of these corrections is known as the Gauss-Bonnet term, first found by Lanczos [9] (therefore it is sometimes referred to as the Lanczos term). In the cosmological context the Lovelock (and Gauss-Bonnet in particular) gravity was intensively studied over the past two decades [10].

In this paper we investigate the dynamics of the flat anisotropic Universe in Lovelock gravity. Since we work in a (4+1)-dimensional case, Lovelock contribution reduces to the Gauss-Bonnet term. We took both the General Relativity (GR) and Gauss-Bonnet (GB) contributions into account for a reason. Namely, with only one of them taken into account, some exact solutions (see, e.g., [11–15]) could be obtained (and that is true not just for GB, but for any order of Lovelock corrections and in any number of dimensions [16]). Though when we take into account different contributions, the equations become much more complicated making it almost impossible to obtain any exact solution in general case (for the first time solutions with both terms taken into account were found in [17]; in [13] a cosmological solution in exponential form was obtained). Yet, the influence of the other (than leading) terms could be significant – for instance, in [12], while investigating a (4+1)-dimensional model with matter in the form of a perfect fluid in a “pure” Gauss-Bonnet case, we discovered an unusual behavior in $w < 1/3$ case, and we believe it was caused by neglecting the GR term in the equations of motion.

The (4+1)-dimensional case with both GR and GB contributions was studied in [18], but a full analysis of all regimes was not performed there. In this paper we are going to do this – we will give a description of all regimes, as well as try to explain some of them analytically.

The second aim of this paper is to investigate the regimes in presence of matter in the form of a perfect fluid. We reported some features of the influence of matter in [13], but no actual description was given. Namely, we reported that the presence of matter leads to an increase of the “probability” of smooth transition between the low- and high-energy Kasner regimes. In the current paper we give a full description of all types of transitions as well as describe the influence of the matter in large. Finally, we generalize the results obtained – both for the vacuum and matter cases – to higher even-dimensional models with all possible Lovelock corrections taken into account.

This article is the logical continuation of [16]. Indeed, in [16] we considered the flat anisotropic cosmological models in the Lovelock gravity, derived the equations of motion and investigated the dynamics with only the highest Lovelock correction taken into account. In this paper we investigate the lowest model ($D = 4$, $n = 2$) with all corrections taken into account and based on the results

predict the behavior of even-dimensional models with all possible Lovelock corrections considered.

II. EQUATIONS OF MOTION

Equations of motion can be easily derived from the general ones, obtained in [16]. In terms of Hubble functions they take a form: dynamical equations

$$\begin{aligned}
& 2(\dot{H}_b + H_b^2) + 2(\dot{H}_c + H_c^2) + 2(\dot{H}_d + H_d^2) + 2H_bH_c + 2H_bH_d + 2H_cH_d + \\
& + 8\alpha \left[(\dot{H}_b + H_b^2)H_cH_d + (\dot{H}_c + H_c^2)H_bH_d + (\dot{H}_d + H_d^2)H_bH_c \right] + p = 0
\end{aligned} \tag{1}$$

(this is the first equation; the rest of them could be obtained via a cyclic indices transmutation) and a constraint equation

$$2H_aH_b + 2H_aH_c + 2H_aH_d + 2H_bH_c + 2H_bH_d + 2H_cH_d + 24\alpha H_aH_bH_cH_d = \rho. \tag{2}$$

In the vacuum case (1) and (2) reduce with $w = 0$ and $\rho = 0$. For simplicity we will refer to the model with a non-zero matter contribution as the “matter case” (or the “matter model”).

So in the matter case in addition to (1) and (2) one also needs an equation of state $p = w\rho$ for the perfect fluid and a continuity equation:

$$\dot{\rho} + (\rho + p)(H_a + H_b + H_c + H_d) = 0. \tag{3}$$

The system (1)–(2) in the vacuum and (1)–(3) in the matter case combined with the initial conditions completely determines the evolution of the Universe as a whole. Hence we are going to solve numerically these equations to find out the future and past evolution of the model with particular initial conditions. Scanning over the initial conditions gives us the needed distribution of regimes.

III. VACUUM MODEL: SPECIAL CASES

Before starting to present the results it would be an asset to consider two special cases that can be found on our transition maps. We call the first of them a 3-equal case with three Hubble parameters

equal to each other. In [18] it was noted that only this regime in a (4+1)-dimensional case has a smooth transition between the low- and high-energy Kasner regimes. Using $H_a = H_b = H_c = H$ and $H_d = h$ the dynamical equations reduce to

$$6H^2 + 4Hh + 4\dot{H} + 16\alpha Hh\dot{H} + 16\alpha H^3h + +2\dot{h} + 2h^2 + 8\alpha H^2h^2 + 8\alpha H^2\dot{h} = 0, \quad (4)$$

$$6\dot{H} + 12H^2 + 24\alpha H^2\dot{H} + 24\alpha H^4 = 0, \quad (5)$$

and the constraint equation gives $h = -H/(1 + 4\alpha H^2)$. Solving (4) and (5) gives

$$\dot{H} = -\frac{2H^2(1 + 2\alpha H^2)}{1 + 4\alpha H^2}, \quad (6)$$

$$\dot{h} = -\frac{2H^2(8\alpha^2 H^4 + 2\alpha H^2 - 1)}{(1 + 8\alpha H^2 + 16\alpha^2 H^4)(1 + 4\alpha H^2)}. \quad (7)$$

Note that our equations are different from those in [18], and we claim ours to be correct¹. Still, the reason why a smooth transition between the low- and high-energy Kasner regimes occurs is the same – the denominator of neither \dot{H} nor \dot{h} never crosses zero.

We call the other case a 2-equal – now only two Hubble parameters are equal to each other. Unlike the 3-equal case, here the denominator of \dot{H}_i can cross zero so a nonstandard singularity could occur. But what is important, in this case there also exists a smooth transition between the low- and high-energy Kasner regimes, thus, the conditions for a smooth transition between the low- and high-energy Kasner regimes are somehow weakened. But since a 2-equal case still needs exact equality, the measure of this transition is not improved.

IV. VACUUM MODEL: RESULTS

As we claimed above, we are going to make a scans over the initial values of Hubble parameters to produce maps of trajectories. Instead of producing 3D maps, as it was done in [18], we will

¹ One can easily verify it – indeed, substituting $H_a = H_b = H_c = H$ into Eq. (7) in [18] (that is the dynamical equation that corresponds to H_d , so it does not have H_d itself but only H_a , H_b , and H_c), one would directly obtain (5); it is quite easy to solve it to obtain (6). The difference might be caused by a wrong sign in $h = -H/(1 + 4\alpha H^2)$ (in [18] the authors have a plus instead of a minus).

make several 2D plots with different values for the third Hubble parameter. Thus the 3-equal case would be a point on our 2D plot with coordinates that coincide with the fixed third Hubble parameter, and the 2-equal case would be a diagonal line and two perpendicular lines with the x - and y -coordinates equal to the fixed third Hubble parameter. So we have three “free” Hubble parameters, the fourth is calculated from the constraint equation (2):

$$H_d^{(0)} = -\frac{H_a^{(0)}H_b^{(0)} + H_a^{(0)}H_c^{(0)} + H_b^{(0)}H_c^{(0)}}{H_a^{(0)} + H_b^{(0)} + H_c^{(0)} + 12\alpha H_a^{(0)}H_b^{(0)}H_c^{(0)}}. \quad (8)$$

Now let us have a look on the denominator of (8). Later, when dealing with the matter case, we will see that this denominator (more specifically, its sign) is an essential thing in describing the matter regimes. For now let us note that if all three Hubble parameters are positive, the denominator is also positive, but if one of the three Hubble parameters is negative, the denominator could be (but not always) negative. We refer to the $(H_a^{(0)}, H_b^{(0)}, H_c^{(0)})$ triplet as a “positive” one if it produces the positive denominator of (8) and as “negative” if it is negative.

Thus we fix the initial value for one of the Hubble parameters (without loss of generality, let it be $H_a^{(0)}$) and scan over $H_b^{(0)}$ and $H_c^{(0)}$ in $[0 \dots 1.5 \div 2]$ range. In previous studies [12, 13, 19] we usually considered $[0, 1]$ range, but now, for the demonstrative reasons we decided to expand it. As for $H_a^{(0)}$, we vary it roughly in $[-1.5 \dots 1.5]$ range. Also, as in all previous studies, we consider only the initially-expanding Universe: $\sum_i H_i^{(0)} \geq 0$. First, we present our results for the positive $H_a^{(0)}$, then for the negative.

Before giving the results, let us summarize what we would expect. For the past evolution, we expect either a standard singularity (high-energy Kasner regime) or a nonstandard one. For the future, there are three possibilities: a low-energy Kasner regime, a recollapse or a nonstandard singularity. For simplicity we denoted them as summarized in Table. With the sign of triplet taken into account, we denote the trajectories like their types with appropriate signs, e.g., type VI+ corresponds to type VI with a positive triplet.

The results for the $H_a^{(0)} > 0$ case are given in Fig. 1. In there, we plotted the resulting past and future behavior for the fixed $H_a^{(0)}$, and with $H_b^{(0)}$ vs. $H_c^{(0)}$ as coordinates. The resulting transitions are denoted according to the Table, the dashed lines are type I trajectories. The value for $H_a^{(0)}$ is increasing from Fig. 1(a) to Fig. 1(f): $H_a^{(0)} = 0.1$ in (a), $H_a^{(0)} = 0.3$ in (b), $H_a^{(0)} = 0.5$ in (c), $H_a^{(0)} = 0.9$ in (d), $H_a^{(0)} = 0.966$ in (e) and $H_a^{(0)} = 1.1$ in (f).

From Fig. 1 one can understand how the transitions evolve with changing $H_a^{(0)}$. At some value –

Table. The classification of possible trajectories in the vacuum (4+1)-dimensional GR+GB model

| From | To | Design. |
|----------------------|--------------------|---------|
| Standard singularity | Kasner | I |
| | Recollapse | II |
| | Non-standard sing. | III |
| Non-standard. sing. | Kasner | IV |
| | Recollapse | V |
| | Non-standard sing. | VI |

in our case with $\alpha = 1$ it occurred at $H_a^{(0)} \approx 0.966$ – two type-IV regions “detach” from each other; with further growth of $H_a^{(0)}$ the bottom-left region shrinks; the upper-right one also decreases in size and moves by diagonal towards the growth of $H_c^{(0)}$ and $H_b^{(0)}$. The $H_a^{(0)}$ value this “detachment” occurs at is dependent on α and governed by a high-order equation, so it is impossible to give it an exact analytical expression.

The $H_a^{(0)} < 0$ case is more complicated than the previous one. Indeed, with all three “free” initial Hubble parameters being positive, the last Hubble parameter is always negative while $\sum_i H_i^{(0)} > 0$ (one can simply verify this from (8)). But with $H_a^{(0)}$ being negative² the situation becomes more complicated. First of all, the calculated Hubble parameter could be either positive or negative. First case is partially epistemologically unimportant to us – this case is equivalent to $H_a^{(0)} > 0$ and thus it does not bring us new regimes, but for the completeness purposes we keep it. The second case could bring new regimes – indeed, with one of the three “free” Hubble parameters being negative, the denominator of (8) could be negative and its regimes, as we will see in the case with a matter source, are distinct from the positive triplets case. However, two negative initial Hubble parameters could also lead to $\sum_i H_i^{(0)} < 0$.

The results are presented in Fig. 2. Therein we gave 2D scans for four different values of $H_a^{(0)}$: $H_a^{(0)} = -0.15$ in (a) panel, $H_a^{(0)} = -0.25$ in (b), $H_a^{(0)} = -0.3$ in (c) and $H_a^{(0)} = -0.5$ in (d). At $H_a^{(0)} \lesssim -0.5$ type-VI trajectories completely “disappear” from the scene, hence we decided to skip the plots of that kind. A white region corresponds to the initial conditions with $\sum_i H_i^{(0)} < 0$; hyperbola-like regions originate from zeros of the denominator in the $H_d^{(0)}$ expression: $H_a^{(0)} + H_b^{(0)} + H_c^{(0)} + 12\alpha H_a^{(0)} H_b^{(0)} H_c^{(0)} = 0$. Thus, the upper-right “half” of the 2D plots in Fig. 2 has a negative denominator of $H_d^{(0)}$ (8) while the others have positive denominators.

² The same with the previous subsection, we fix $H_a^{(0)}$ and plot 2D figs with $H_b^{(0)}$ and $H_c^{(0)}$ as the x - and y -coordinates.

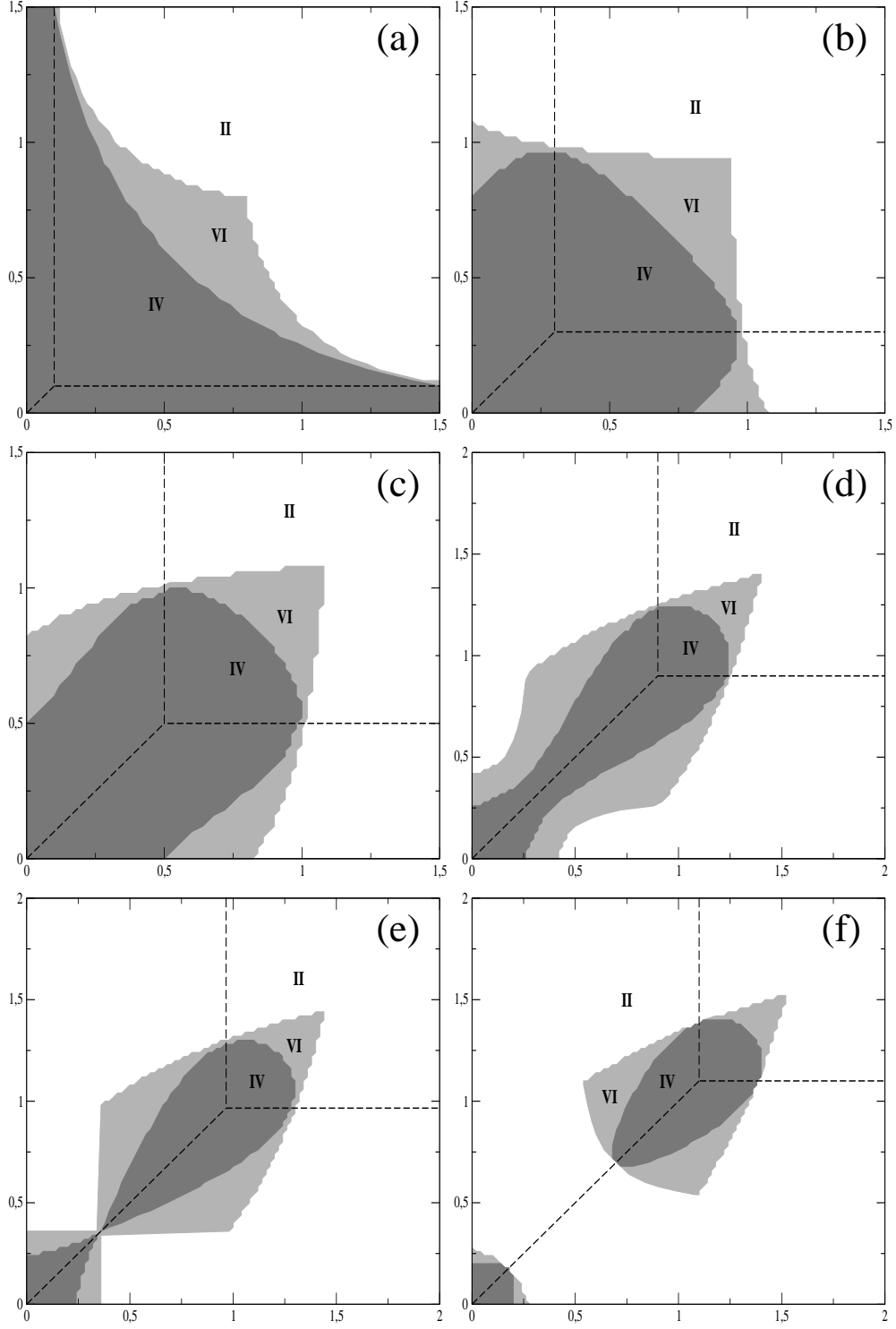


FIG. 1: Transitions for $H_a^{(0)} > 0$ in the vacuum case. The $H_a^{(0)}$ value is increasing from (a) to (f). Trajectory types are denoted according to the Table. Dashed lines correspond to the type-I trajectories.

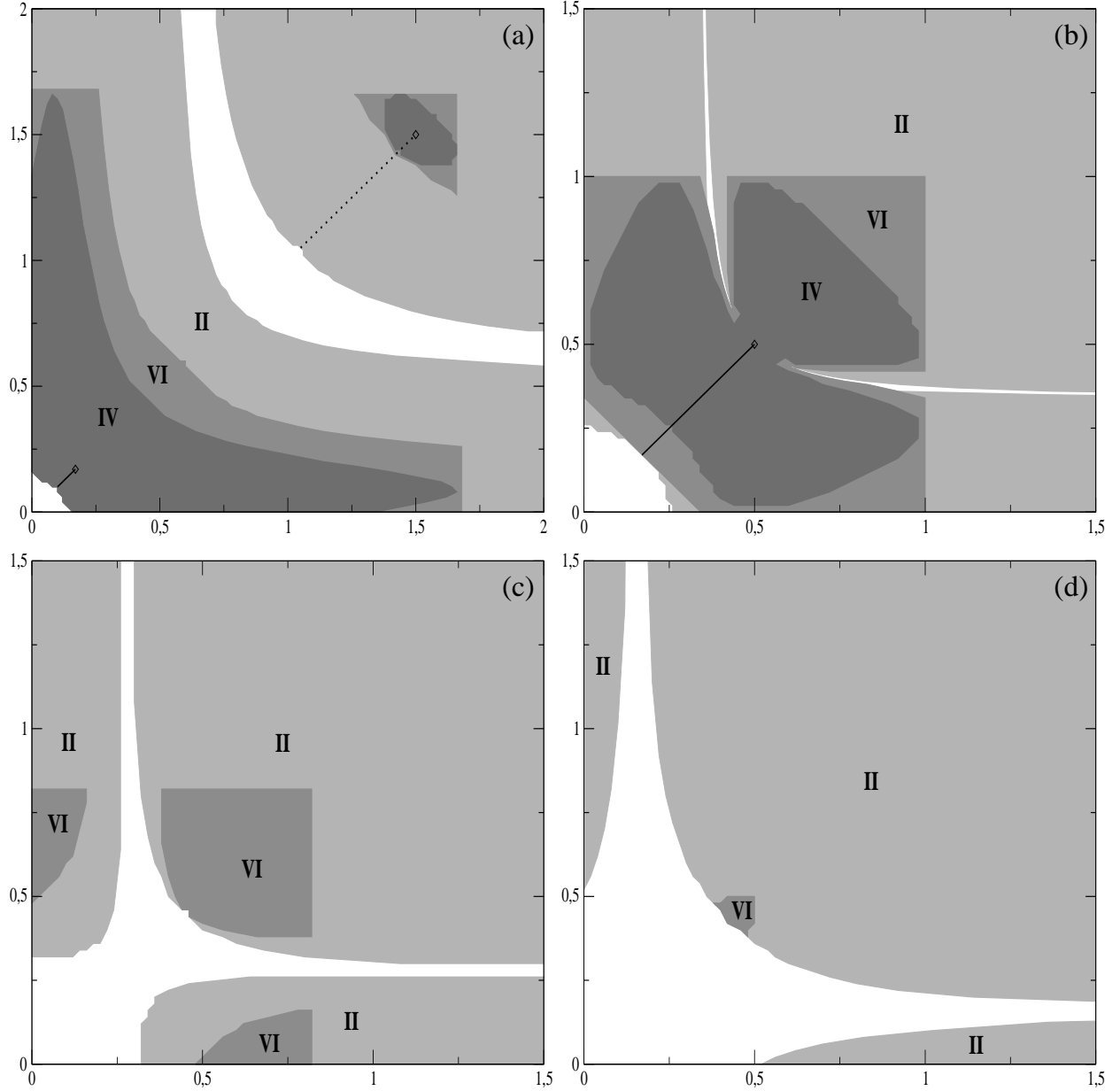


FIG. 2: Transitions for $H_a^{(0)} < 0$ in the vacuum case. The $H_a^{(0)}$ value is decreasing ($|H_a^{(0)}|$ is increasing) from (a) to (d). Trajectory types are denoted according to the Table. Solid lines correspond to the I+ trajectories, dotted – to the I–.

In addition to the type II, IV, and VI trajectories at low values of $|H_a^{(0)}|$, one can find type-I trajectories as well. There as well exists the transition of I– type, that we can call “the rarest” trajectory. Indeed, it exists only at $H_a^{(0)} < 0$, only at 2-equal lines, at low enough $|H_a^{(0)}|$ (type-IV should not disappear yet $-H_a^{(0)} > -1/(4\sqrt{\alpha})$), and on the upper “half” of the plot; the I–

trajectories are denoted by a dotted line in Fig. 2(a). The I+ transitions are denoted as solid lines in Fig. 2(a) and (b). One can see that type-I trajectories exist between the lower boundary of the $\sum_i H_i^{(0)} > 0$ and some point that we denoted as diamonds in Fig. 2(a) and (b). These points correspond to the 3-equal situation: indeed, from Sec. III we remember that in the 3-equal regime the calculated Hubble parameter is always negative. If we assume $H_a^{(0)}$ to be that parameter, then the 3-equal situation occurs at

$$H_b^{(0)} = H_c^{(0)} = H_d^{(0)} = -\frac{1}{8} \frac{1 \pm \sqrt{1 - 16\alpha(H_a^{(0)})^2}}{\alpha H_a^{(0)}}. \quad (9)$$

Two different 3-situations are infinitely separated at $H_a^{(0)} \rightarrow (0-0)$, become closer with the growth of $|H_a^{(0)}|$ and coincide when $H_a^{(0)} = -1/(4\sqrt{\alpha})$ (with $\alpha = 1$ it happened at $H_a^{(0)} = -0.25$; the situation is presented in Fig. 2(b)).

V. VACUUM MODEL: DISCUSSION

In the first half of the article we dealt with the vacuum (4+1)-dimensional flat anisotropic model in the Einstein-Gauss-Bonnet gravity. One can see that the type-II trajectories are dominating in both $H_a^{(0)} > 0$ and $H_a^{(0)} < 0$ situations; in other words, the type-II trajectories are dominating all other regimes in the model considered. In the $H_a^{(0)} > 0$ case we have IV and VI-type trajectories more or less abundant, their presence is in general lessened with the growth of $H_a^{(0)}$, but they never vanish. In the $H_a^{(0)} < 0$ case the situation is more dramatic: with small $|H_a|$ we have I, II, IV, and VI type trajectories, but with the growth of $|H_a|$ we first “loose” I and IV, then VI, therefore finally at $H_a^{(0)} \lesssim -0.5$ (with $\alpha = 1$; with a different value for α this will happen at another value for the $H_a^{(0)}$) we have only type-II transitions.

In Fig. 3 we presented the examples of all the possible transitions. Black curves correspond to the expansion rate in terms of the Hubble parameters $\sum_i H_i$, and grey curves represent the value for the denominator of the \dot{H}_i expression. Time is along x -axis and is normalized in a way to set $\alpha = 1$; zero-point $t = 0$ corresponds to the start of integration. Type I is in (a), II – (b), IV – (c), and VI – (d). Hence there are no type-III and V transitions, and now we will try to explain why. One can see that the nonstandard singularity occurs only in the vicinity of the standard one (but it is not necessary that it will happen – see Fig. 3(a) for example). From Figs. 3(a) and (c) one can learn that the trajectories, starting from the positive values of the denominator end up in

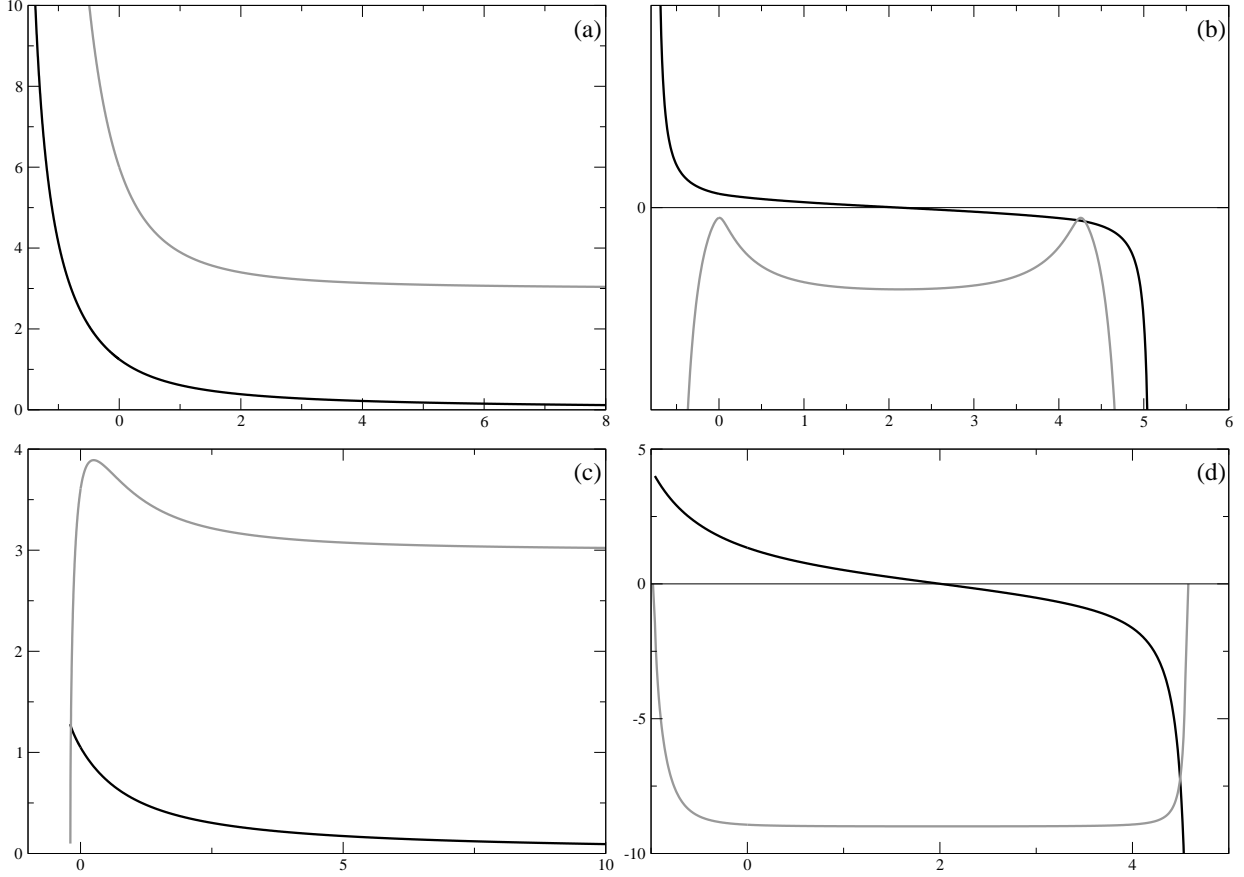


FIG. 3: Examples of different type of transitions. Black curve is the expansion rate in terms of the Hubble parameters $\sum_i H_i$, grey curve is the value for the denominator in the \dot{H}_i expression. Type I is in (a), II – (b), IV – (c), and VI – (d).

the Kasner regime. We checked that for the scans in Fig. 1, and found that the type-IV regime completely coincides with an initially positive denominator. The reason behind this link between the positivity of denominator and the late-time Kasner behavior is a bit aside from the goals of this paper and is yet to uncover – we are going to devote a separate paper to the nonstandard singularity in flat anisotropic models in the Lovelock gravity. Anyway, type III and V trajectories cannot originate from the positive initial value of the denominator. As for the negative value, the remaining two possibilities are presented in Figs. 3(b) and (d). One could think of the possibility for the type-III trajectory to occur on the singular analog of the left branch in Fig. 3(b) – on the short “window” between the standard and nonstandard singularities, but our numerical analysis demonstrated that it is not happening. We believe this situation could not even be constructed: crossing the nonstandard singularity changes the sign of the denominator leaving the numerator

unchanged; thus at this point the sign of \dot{H}_i changes, making it useless to try to construct any continuation beyond the nonstandard singularity.

VI. MODEL WITH MATTER

In this section we start our investigation of the models filled with matter in the form of a perfect fluid. In this case the constraint equation gives us a bit different expression for the 4th Hubble parameter:

$$H_d^{(0)} = -\frac{2H_a^{(0)}H_b^{(0)} + 2H_a^{(0)}H_c^{(0)} + 2H_b^{(0)}H_c^{(0)} - \rho_0}{2H_a^{(0)} + 2H_b^{(0)} + 2H_c^{(0)} + 24\alpha H_a^{(0)}H_b^{(0)}H_c^{(0)}}. \quad (10)$$

From (10) one can easily see that the expression for $H_d^{(0)}$ is split into two parts – ρ -dependent and ρ -independent. The latter remains the same with varying ρ while the former changes the value for $H_d^{(0)}$. At this point the positive and negative triplets start to play an important role. These two have a huge difference – the positive triplets have no boundary on the density while the negative do. Indeed, keeping in mind that $\sum H_i^{(0)} \geq 0$ and the fact that the increasing density decreases $H_d^{(0)}$, even if at $\rho = 0$ we have $\sum H_i^{(0)} > 0$, at some value for ρ we will have $\sum H_i^{(0)} = 0$. This difference between the positive and negative triplets affects the details of their regimes, so while describing the regimes we will describe them separately.

VII. MODEL WITH MATTER: RESULTS

Now let us describe the matter regimes. The first one to describe is I+ case. In the vacuum case, only I+ and I– have the smooth transition from the standard singularity to the Kasner expansion, but, as we noted in [13], in the model with matter it is no longer the case. In the presence of matter the transition remains unchanged: it is from the standard singularity to the expansion. The difference between the $w < 1/3$ and $w > 1/3$ cases lies in the isotropisation: at $w > 1/3$ the initial singularity becomes isotropic (and the expansion is the GR-dominated Kasner) while at $w < 1/3$ we have a standard GB-dominated singularity and an isotropic expansion.

Trajectories of I– type, as we already mentioned, are “the rarest” trajectories. In the presence of matter the regimes changes according to Fig. 4(a); the trajectory types are denoted in the figure.

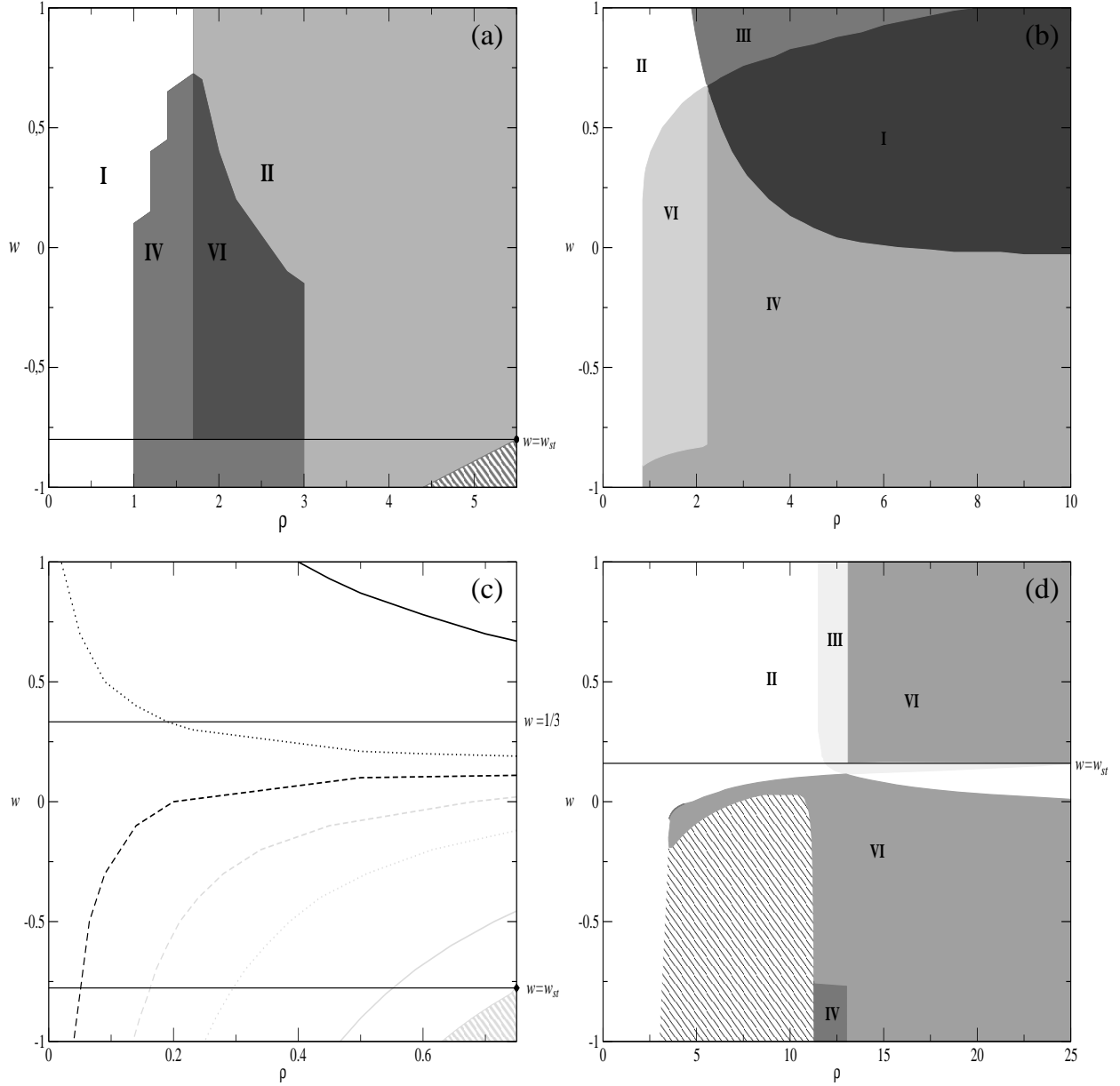


FIG. 4: An example trajectory map in (ρ, w) coordinates for I- (a), II+ (b) and II-: $w_{st} < 0$ (c) and $1/3 > w_{st} > 0$ (d) subcases. The stroked region in (a), (c), and (d) panels corresponds to the periodical trajectories reported in [13]. See the text for details.

As a regime with the negative triplet, it has the maximal value for density; the x -axis of the Fig. 4(a) covers all possible values for density.

The transitions in the (ρ, w) map for II+ type trajectory are given in Fig. 4(b). There is a difference between the regimes at $w < 1/3$ and $w > 1/3$: in the $w < 1/3$ case, the GR-Kasner

“transforms” into an isotropic expansion while in the $w > 1/3$ case, the isotropic one is the initial singularity.

From Fig. 4(b) one can easily see what brings an addition of matter to this regime. First of all, new, unknown for the vacuum case, type-III regime is introduced. It doesn’t cover a wide range of ρ and w , but its presence is still important. Secondly, the type-I trajectory in this case is unbounded from high densities. Thus, we find that the presence of matter in the form of a perfect fluid makes the type-I transition common in terms of initial parameters in contrast with the vacuum case, where one requires fine-tuning to achieve this regime. One can also notice that the type-I transition covers both $w > 1/3$ and $w < 1/3$ cases, so the expansion can be both Kasner-type and isotropic, respectively. Finally, the region of type-IV trajectories is also unbounded from high densities and lies mostly in the lower half of the (ρ, w) map; later we will see that this is more or less typical for the type-IV trajectories.

The II– case is more complicated than the others. Namely, it has a different behavior in the $w_{st} < 0$ and $1/3 > w_{st} > 0$ cases. We consider them separately, and now we only note one feature of the $w > 1/3$ regimes: the initial singularity is GR-dominated in contrast with I+ and II+ where in the $w > 1/3$ case the initial singularity was isotropic.

In $w_{st} < 0$ case almost all the trajectories remain the same – II type. Since this is “standard singularity \rightarrow recollapse”, one can find its “lifetime”. To demonstrate the influence of matter on the dynamics, we plotted the resulting lifetimes on the (ρ, w) map (see Fig. 4(c)). The stroked region in the bottom-right corner marks the positions of periodic trajectories – a new type of solution in the vicinity of the stationary one ($\rho = \rho_{st}$, $w = w_{st}$), described in [13]. Also one can notice that there is no abrupt difference between the $w < 1/3$ and $w > 1/3$ regimes.

And one last point regarding this regime – in the case of $w_{st} < -1$ (this is possible in some triplets) we do not have anymore periodical trajectories (and so only type II trajectories remains) as they are all located at $w < -1$ which is beyond physical assumptions.

The case with $1/3 > w_{st} > 0$ is different from the described above $w_{st} < 0$ – it has more different regimes. In Fig. 4(d) we presented the map of transitions in (ρ, w) coordinates.

The map of trajectories for the IV+ case is given in Fig. 5. There in panel (a) we present a large-scale structure of the transitions; in panel (b) – a detailed structure of the boundary between I and IV at low densities and in panel (c) – the boundary between I and IV at large.

The resulting (ρ, w) transition map for the IV– case is given in Fig. 6(a). The type IV trajec-

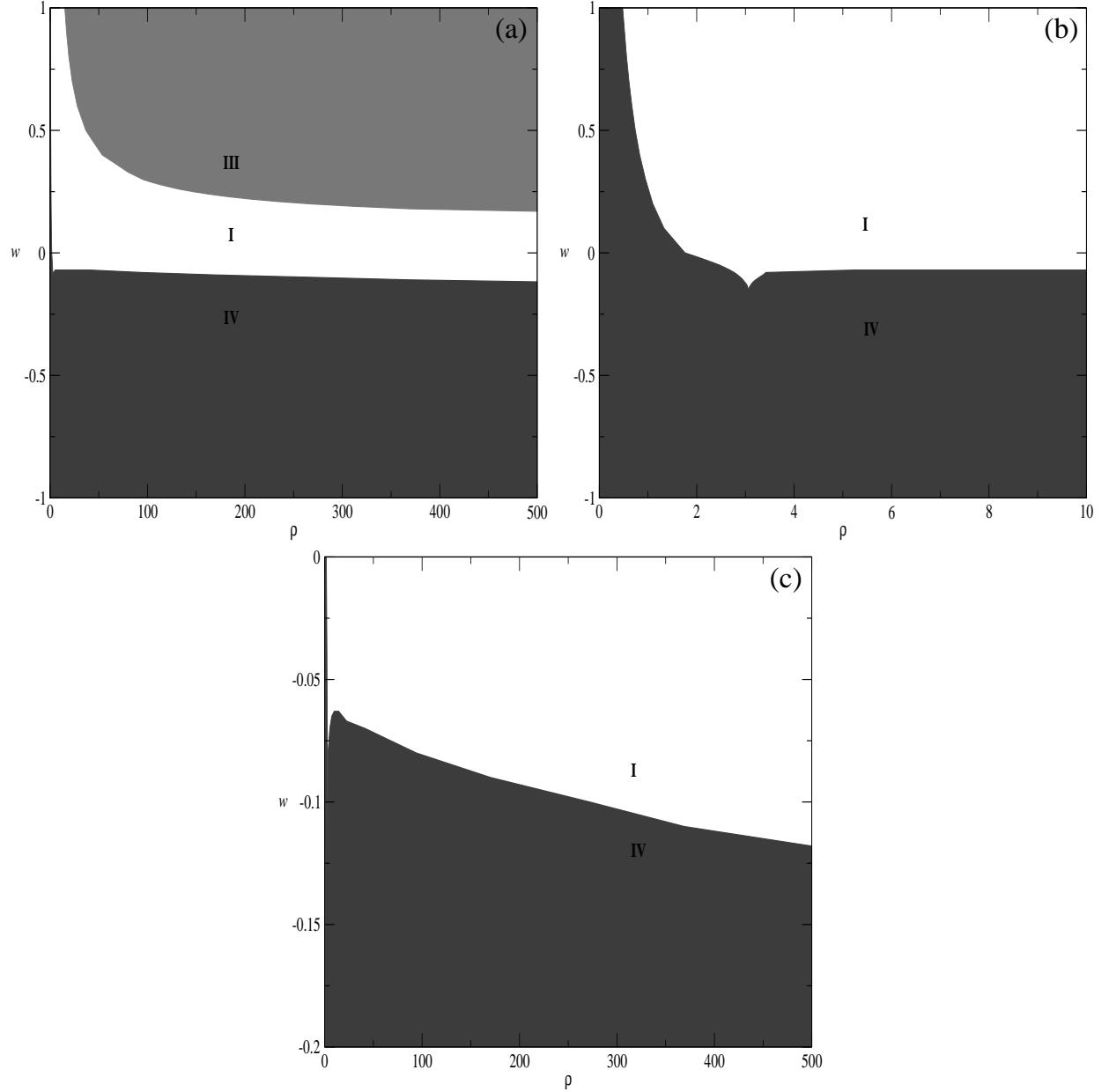


FIG. 5: An example trajectory map in the (ρ, w) coordinates for the IV+ case. In (a) we can see the large-scale structure of the transitions (up to very large values of ρ), in (b) we presented the boundary between I and IV at low densities with feature, and finally in (c) – the boundary between I and IV at large.

jectories are quite bounded in there, but we have another regime, unseen in the vacuum case – type V. With it we have all the six possible regimes in the presence of matter. With high enough w_{st} we have a relatively large area with periodic trajectories.

Two final regimes, $\underline{\text{VI}}_+$ and $\underline{\text{VI}}_-$, are presented in Figs. 6(b), (c), and (d). In Fig. 6(b) we

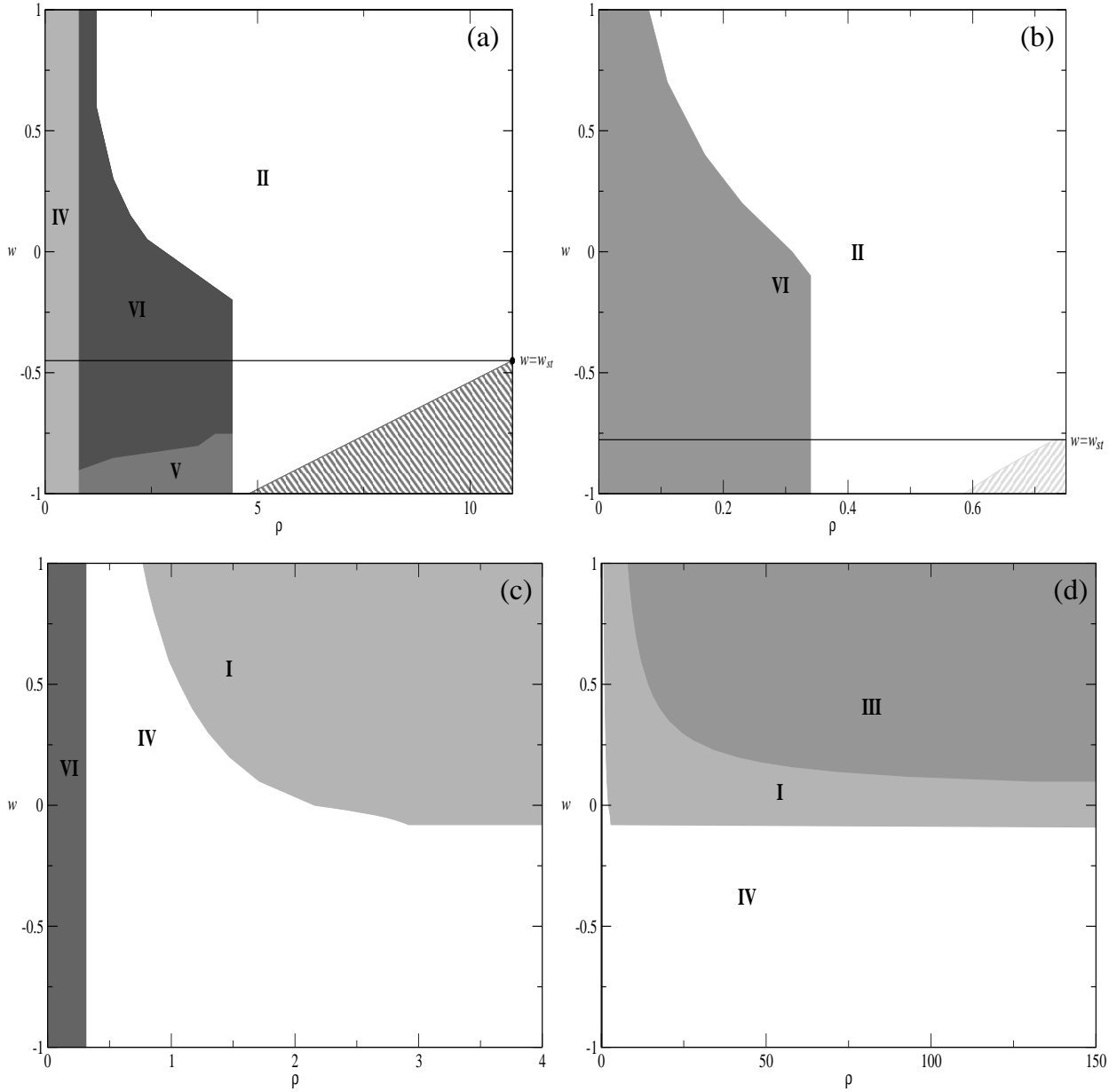


FIG. 6: (a) Example of the (ρ, w) transition map for the IV– case; (b) – the same but for the VI– case. One can see the region with periodical trajectories in the bottom-right corner of panels (a) and (b). In (c) and (d) panels – (ρ, w) transition map for the VI+ case: structure at low ρ in (c) and large-scale structure in (d).

presented type VI– and in Figs. 6(c) and (d) – type VI+: the behavior at low values for ρ in (c) and the large-scale structure of the transitions in (d).

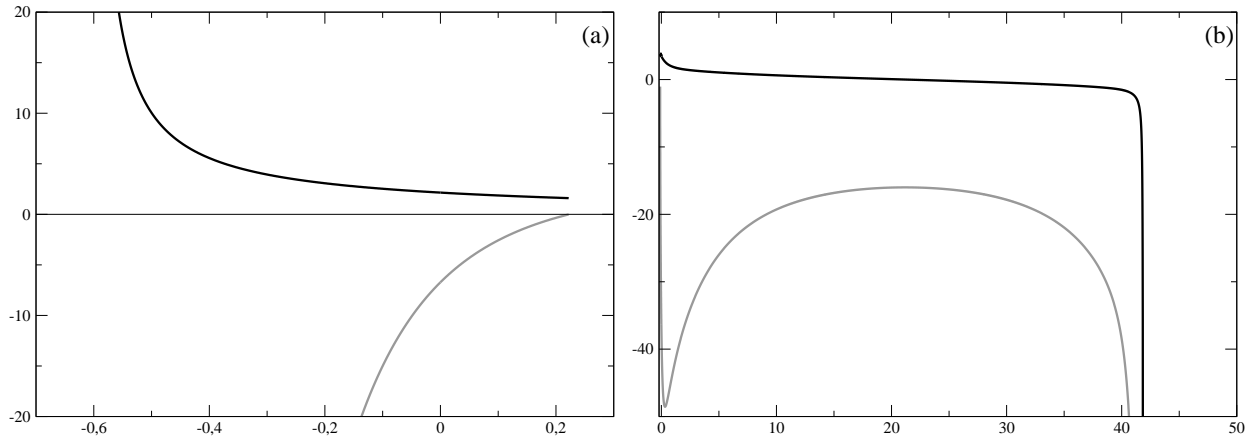


FIG. 7: Type-III (a) and type-V (b) transitions in the case with matter. Black line represent $\sum H_i$, grey – denominator of \dot{H} expression.

VIII. MODEL WITH MATTER: DISCUSSION

In the second part of the paper we studied what influence the matter in the form of a perfect fluid exerts upon the dynamics of flat (4+1)-dimensional anisotropic models in the Einstein-Gauss-Bonnet gravity. One of the two main changes from the vacuum case is a substantial increase of the type-I transitions we previously reported in [13]. An interesting feature – only positive triads have type-I transition in the presence of matter, negative (with an exception of I–) do not. In this paper we demonstrate this increase “quantitatively”. Another feature is the appearance of type-III and type-V trajectories. First of them appeared exactly the way we discussed in the vacuum case: on the singular analog of the left branch of Fig. 3(b). We presented both III and V in Fig. 7³. Thus, the presence of matter changes the dynamics to make such trajectories to exist.

One can find different “features” on the (ρ, w) transition maps and most of them (those that are unrelated to w_{st}) are just triplet-specific features. A feature at the II+ transition map (Fig. 4(b)) where all five regimes “touch” is a good example. If we draw a $w = \text{const}$ line from that point to $\rho = 0$ we will notice that the lifetimes for type-II trajectories along this line are the same and equal to that of the vacuum case. It is obvious that the lifetime in the vacuum case is triplet-specific and varies from triplet to triplet, hence the location of features of that type also varies from triplet to triplet. The same situation is with the features of other kinds.

³ Remarks to Fig. 3 regarding the time are valid to Fig. 7 as well.

Now we want to draw your attention to the II– $1/3 > w_{st}$ case. One can see that it is very different from other cases. It has periodical trajectories at an “unusual” (from the other regimes that have periodical trajectories) place and it has much more type-VI transitions than the other regimes do. The reasons behind this behavior are not clear; probably, that is due to crossing the “special solution” $w = 0$, found in [12] numerically for the GB+matter case (later in [16] we demonstrated that this is a general feature for all even-dimensional flat anisotropic models in the Lovelock gravity with only the higher-order correction taken into account).

One can notice that generally, inside a triplet, the transition maps have a lot in common. For the positive triplet we have III→I→IV “regimes stratification” (over w) on large ρ : in the II+ case (Fig. 4(b)), we have the same situation in IV+ (Fig. 5) and VI+ (Fig. 6(c, d)). In the II+ case type-III trajectory “disappears” at some density, but that is just an effect of a particular triplet: in another triplet with a lower value for w at which the feature occurs we will have all the three regimes at high densities. Negative triplets also have some features in common. They all have type-II at the intermediate and high values of density and, if $w_{st} > -1$, they have periodical trajectories. They all as well (except II–) have type-VI at low–intermediate values of density.

Therefore we see that the positive triplets have a high-density regime stratification over w while the negative triplets have it over the density itself. Keeping in mind the difference between the triplets one can explain this: for negative triplets the density is more important – high density can cause $\sum_i H_i^{(0)} < 0$, so the value for density determines initial regimes. For positive triplets all values of density are acceptable hence the role of density is less important and the equation of state determines the regimes.

IX. HIGHER-DIMENSIONAL CASES

Finally, as we claimed at the beginning, we are going to generalize the obtained results on the higher-dimensional flat anisotropic models in the Lovelock gravity. First of all, in [16] we obtained the equations of motion for the flat anisotropic cosmological model in the Lovelock gravity in any number of dimensions with only the highest possible correction taken into account. We also demonstrated how one can obtain the equations for the mixture of corrections. If we take into account all possible corrections, the resulting equations for different orders would have a similar structure, and so would the solutions. Therefore we expect the II-type trajectories to dominate in all the even-dimensional models. The negative multiplets (the analogs of triplets from (4+1))

would as well have a more complicated structure than that in Fig. 2. This is caused by more possible zeros of the denominator of the calculated Hubble parameter. In its turn, it will increase the effective presence of type-I, IV, and VI trajectories. The gain in type-I is also due to the increase of possible $(D - k)$ -equalities, but still the measure will be incomparable with other types of regimes.

We do not expect any changes in the negative multiplets – they are governed by the density – but there might be changes in the positive multiplets. Indeed, they are governed by the equation of state, and its influence is dependent on the number of dimensions. The equation of state that corresponds to the highest possible contribution (n -order) is $w_{eq} = 1/(2n - 1)$. With the growth of n we have $w_{eq} \rightarrow (0 + 0)$; as one of the consequences one would expect a decrease of the presence of the II– type trajectory with $0 < w_{st} < w_{eq}$ – the corresponding range of w would shrink eventually decreasing the presence. As another consequence one would expect a decrease of the type-I presence in the positive multiplets (apart from I– we do not have type-I in the negative triplets in $(4+1)$). This is caused by the same “shrinking” $w_{eq} \rightarrow (0 + 0)$ while $w = 0$ is the “special solution” for the even-dimensional case [16]. Thus the region $0 < w < 1/3$ from $(4+1)$ (where the type-I trajectories are located) with the growth of n would shrink resulting in a decrease of presence of the type-I transitions.

Also, the characteristic scale of the Hubble parameters where types I, IV, and VI occur will drop with the growth of n . This is due solely to the number of dimensions – indeed, the same amount of matter produces lower density in the higher dimensions. Our calculations for $D = 6$ and $D = 8$ confirmed that. Thus, purely due to the growth of n the effective presence of the type-I, IV, and VI trajectories is decreasing.

X. CONCLUSIONS

In this paper we gave the first complete description of all the regimes in the $(4+1)$ -dimensional flat anisotropic cosmological model in the Einstein-Gauss-Bonnet gravity. All through the paper we hold the condition on the initial values of Hubble parameters: $\sum H_i^{(0)} > 0$. With the $\sum H_i^{(0)} < 0$ case taken into account, our description will be complete. And the $\sum H_i^{(0)} < 0$ case could be easily obtained from the $\sum H_i^{(0)} > 0$ case: indeed, assuming $\sum H_i^{(0)} < 0$ we effectively only make a $t \rightarrow -t$ transform, so we will have the same, but time-reversed results, such as, “standard singularity \rightarrow Kasner” turns into “Kasner \rightarrow recollapse” and so on. With this remark in mind, our description

of the regimes is complete for all the possible values of the initial Hubble parameters.

We have found that the type-II transition (“standard singularity \rightarrow recollapse”) dominates over all the other types of trajectories in the vacuum case, and describe it both qualitatively and quantitatively. We as well found that the type-I transition (“standard singularity \rightarrow Kasner regime”) is spread more widely than it was assumed [18], but still not enough to compete even with type IV.

If we add matter in the form of a perfect fluid, the situation changes drastically. Not only the abundance of the type-I transition becomes comparable with abundances of other types [13], but we also obtain new regimes that are unknown for the vacuum case⁴ (type-III and V). With these two, in the matter case we have all the possible transitions between two possibilities for the past (standard and nonstandard singularities) and three for the future (the Kasner regime, recollapse and nonstandard singularity) evolutions. We gave the description of the influence of matter on all the initially possible vacuum regimes.

Apart from the description of the matter regimes, we found that at intermediate–high densities all the regimes (inside their triplet) look alike: positive triplets have III \rightarrow I \rightarrow IV “regime stratification” (with a decrease of w) while negative ones have VI \rightarrow II “regime sequence” (with an increase of ρ). Thus, the influence of matter is stronger than we anticipated: it does not just significantly increase the abundance of the type-I transition and adds the two remaining possible trajectories, but also almost “erases the bounds” between different trajectories inside the triplet. But there are exceptions like II– with $0 < w_{st} < 1/3$ that we discussed in the relevant section.

Finally we generalized the obtained results on the higher-dimensional case. We expect that the vacuum even-dimensional flat anisotropic models in the Lovelock gravity of the n order are dominated by the type-II transition. The presence of the other types of transitions is in general more and more suppressed with the growth of n . The presence of matter acts the same (as described for (4+1)) way in the case of negative multiplets and the same but with decreases of the presence of type-I trajectories with the growth of n in the case of positive multiplets. Therefore, the even-dimensional vacuum models are degenerative from the point of view of the presence of a smooth transition between the standard singularity and the cosmological expansion; the presence of matter in the form of a perfect fluid lifts this degeneration but with the growth of n this improvement

⁴ Let us note – considering the $\sum H_i^{(0)} < 0$ case would not bring these two cases for they are time-reversal to each other.

decreases. Let us note, though, that $(2 + 1)$ in L_1 differs from the described above picture [20]; hence, the analysis is valid only at $n \geq 2$.

-
- [1] G. Nordström, Phys. Z. **15**, 504 (1914)
 - [2] T. Kaluza, Sit. Preuss. Akad. Wiss. **K1**, 966 (1921).
 - [3] O. Klein, Z. Phys. **37**, 895 (1926).
 - [4] M. Green, J. Schwarz, and E. Witten, *Superstrings* (Cambridge University Press, Cambridge, England, 1987).
 - [5] N. Arkani-Hamed, S. Dimopoulos, and G. Dvali, Phys. Lett. B **429**, 293 (1998); I. Antoniadis, N. Arkani-Hamed, S. Dimopoulos, and G. Dvali, Phys. Lett. B **436**, 257 (1998); N. Arkani-Hamed, S. Dimopoulos, and G. Dvali, Phys. Rev. D **59**, 086004 (1999).
 - [6] P. Horava and E. Witten, Nucl. Phys. B **460**, 506 (1996); *ibid.* **475**, 94 (1996).
 - [7] H.-Ch. Cheng, arXiv:1003.1162; T. Rizzo, arXiv:1003.1698.
 - [8] D. Lovelock, J. Math. Phys. **12**, 498 (1971).
 - [9] C. Lanczos, Z. Phys. **73**, 147 (1932); C. Lanczos, Ann. Math. **39**, 842 (1938).
 - [10] F. Müller-Hoissen, Phys. Lett. **163B**, 106 (1985); J. Madore, Phys. Lett. **111A**, 283 (1985); J. Madore, Class. Quant. Grav. **3**, 361 (1986); F. Müller-Hoissen, Class. Quant. Grav. **3**, 665 (1986); B. Zumino, Phys. Rep. **137**, 109 (1986); N. Deruelle, Nucl. Phys. **B327**, 253 (1989); T. Verwimp, Class. Quant. Grav. **6**, 1655 (1989); G. A. Mena Marugán, Phys. Rev. D **42**, 2607 (1990); *ibid.* **46**, 4340 (1992); N. Deruelle and L. Fariña-Busto, Phys. Rev. D **41**, 3696 (1990); J. Demaret et al., Phys. Rev. D **41**, 1163 (1990); M. Farhoudi, Gen. Rel. Grav. **41**, 117 (2009).
 - [11] I. V. Kirnos and A. N. Makarenko, arXiv:0903.0083.
 - [12] I.V. Kirnos, A.N. Makarenko, S.A. Pavluchenko, and A.V. Toporensky, arXiv:0906.0140.
 - [13] I.V. Kirnos, S.A. Pavluchenko, and A.V. Toporensky, arXiv:1002.4488.
 - [14] V. D. Ivashchuk, arXiv:0909.5462.
 - [15] V. D. Ivashchuk, arXiv:0910.3426.
 - [16] S.A. Pavluchenko, Phys. Rev. **D80**, 107501 (2009) // arXiv:0906.0141.
 - [17] D. G. Boulware and S. Deser, Phys. Rev. Lett. **55**, 2656 (1985).
 - [18] R. Chingangbam, M. Sami, P. V. Tretyakov, and A.V. Toporensky, Phys. Lett. **B661**, 162 (2008) // arXiv:0711.2122.
 - [19] S.A. Pavluchenko and A.V. Toporensky, Mod. Phys. Lett. **A24**, 513 (2009) // arXiv:0811.0558.
 - [20] S. Giddings, J. Abbott, and K. Kuchař, Gen. Rel. Grav. **16**, 751 (1984).